AD-A041 313 FLOW RESEARCH CO KENT WASH F/G 20/4
OPTIMIZATION OF LOW-DRAG BODIES OF REVOLUTION WITH TURBULENT BO--ETC(U)
APR 77 E W GELLER, J E MERCER, R W METCALFE N00014-75-C-0425
UNCLASSIFIED FLOW-RR-79 NL

| OF |
AD
A041313

END

DATE
FILMED
7-77

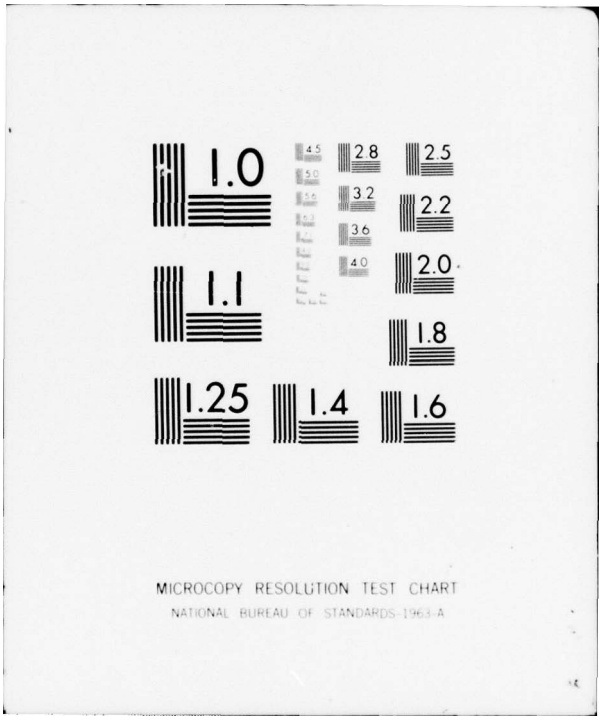
1.0
1.1
1.25
1.4
1.6
1.8
2.0
2.2
2.5
2.8
3.2
3.6
4.0
4.5
5.0
5.6
MICROCOPY RESOLUTION TEST CHART
NATIONAL BUREAU OF STANDARDS-1963-A

12

FLOW RESEARCH COMPANY

A DIVISION OF FLOW INDUSTRIES, INC.

HEADQUARTERS
P.O. Box 5040, 21414 - 68th Ave. S.
Kent, (Seattle), WA 98031 (206) 854-1370
Seattle Ex. 622-1500 TWX 910-447-2762

PRINCETON COMBUSTION LABS
P.O. Box 237
Plainsboro, NJ 08536
(609) 452-9200

EUROPE
53 Barton Rd., Blechley
Milton Keynes MK23B1 England
MK0908 71571/71572 Telex 826671

FLOW RESEARCH REPORT NO. 79

OPTIMIZATION OF LOW-DRAG BODIES OF REVOLUTION WITH TURBULENT BOUNDARY LAYERS*

BY

EDWARD W. GELLER
JOHN E. MERCER
RALPH W. METCALFE
EARLL M. MURMAN

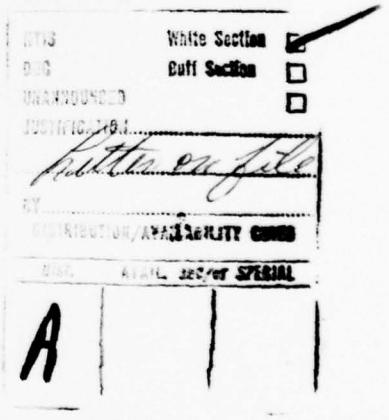

APRIL 1977

FLOW RESEARCH COMPANY
A DIVISION OF FLOW INDUSTRIES, INC.
P.O. Box 5040
KENT, WASHINGTON 98031
(206) 854-1370

*This work was sponsored by the Office of Naval Research under ONR Contract No. N00014-75-C-0425 (NR 061-227/10-29-74 438). Reproduction in whole or in part is permitted for any purpose of the United States Government.

(14) Flow-RR-79

SECURITY CLASSIFICATION OF THIS PAGE (When Data Entered)

REPORT DOCUMENTATION PAGE

READ INSTRUCTIONS BEFORE COMPLETING FORM

1. REPORT NUMBER: Flow Research Report No. 79
2. GOVT ACCESSION NO.: (9) Final rept. 15 Dec 74-14 Feb 77
3. RECIPIENT'S CATALOG NUMBER:

4. TITLE (and Subtitle): (6) Optimization of Low-Drag Bodies of Revolution With Turbulent Boundary Layers.
5. TYPE OF REPORT & PERIOD COVERED: Final 12/15/74 - 2/14/77
6. PERFORMING ORG. REPORT NUMBER:

7. AUTHOR(s): (10) Edward W. Geller, John E. Mercer, Ralph W. Metcalfe and E. M. Murman
8. CONTRACT OR GRANT NUMBER(s): (15) N00014-75-C-0425

9. PERFORMING ORGANIZATION NAME AND ADDRESS: (1) Flow Research Company, P.O. Box 5040, (2) Kent, Washington 98031
10. PROGRAM ELEMENT, PROJECT, TASK AREA & WORK UNIT NUMBERS:

11. CONTROLLING OFFICE NAME AND ADDRESS: Office of Naval Research, 800 North Quincy Street, Arlington, VA 22217
12. REPORT DATE: April 1977
13. NUMBER OF PAGES: 42 (12) 44p.

14. MONITORING AGENCY NAME & ADDRESS (if different from Controlling Office): Defense Contract Administration Services, Naval Support Activity, Building 5D, Seattle, WA 98115
15. SECURITY CLASS. (of this report): Unclassified
15a. DECLASSIFICATION DOWNGRADING SCHEDULE:

16. DISTRIBUTION STATEMENT (of this Report)

DISTRIBUTION STATEMENT A
Approved for public release;
Distribution Unlimited

Scientific Officer N00014 (1 copy)
Cognizant ONR Branch Office N62887 (1 copy)
Administrative Contracting Officer S4801A (1 copy)
Director, U.S. Naval Research Laboratory N00173 Washington D.C. 20375
Code 2629 (6 copies) Code 2627 (6 copies)
Defense Documentation Center, Bldg. 5, Cameron Station, Alexandria, VA (12)

17. DISTRIBUTION STATEMENT (of the abstract entered in Block 20, if different from Report)

18. SUPPLEMENTARY NOTES

19. KEY WORDS (Continue on reverse side if necessary and identify by block number)

low drag bodies
optimization
drag coefficient

20. ABSTRACT (Continue on reverse side if necessary and identify by block number)

Numerical optimization methods are used to search for minimum-drag bodies of revolution in incompressible flow with all-turbulent boundary layers. Available methods for potential flow, boundary layer, drag, and optimization calculations are used. Results obtained with an empirical drag formula give a low-fineness ratio body with significantly lower drag than for traditional shapes. However, when the drag method of Nakayama and Patel is used as a representative state-of-the-art capability, results show that the drag is insensitive to perturbations from the shape of traditional bodies, and only a small reduction in drag is obtained.

DD FORM 1 JAN 73 1473 EDITION OF 1 NOV 65 IS OBSOLETE

SECURITY CLASSIFICATION OF THIS PAGE (When Data Entered)

390 409

Flow Research Report No. 79
April 1977

Optimization of Low-Drag Bodies of Revolution With Turbulent Boundary Layers*

by

E. W. Geller, J. E. Mercer, R. W. Metcalfe, and E. M. Murman
Flow Research Company, Kent, Washington 98031

Abstract

Numerical optimization methods are used to search for minimum-drag bodies of revolution in incompressible flow with all-turbulent boundary layers. Available methods for potential flow, boundary layer, drag, and optimization calculations are used. Results obtained with an empirical drag formula give a low-fineness-ratio body with significantly lower drag than for traditional shapes. However, when the drag method of Nakayama and Patel is used as a representative state-of-the-art capability, results show that the drag is insensitive to perturbations from the shape of traditional bodies, and only a small reduction in drag is obtained.

*This work was sponsored by the Office of Naval Research under ONR Contract No. N00014-75-C-0425 (NR 061-227/10-29-74 438). Reproduction in whole or in part is permitted for any purpose of the United States Government.

Table of Contents

Nomenclature

Symbol	Definition
A	reference area for the drag coefficient
a_i	the i^{th} parameter defining the body shape
C_D	drag coefficient
C_{D_f}	skin-friction drag coefficient
C_{D_p}	pressure drag coefficient
C_{D_V}	$\frac{D}{\frac{1}{2}\rho U_\infty^2 V^{2/3}}$, drag coefficient based on the body volume
C_f	skin-friction coefficient
D	body drag
$\mathcal{D}$	maximum body diameter
H	$\frac{\Delta_2}{\Delta_1}$, boundary layer shape factor
$\overline{H}$	$\frac{\overline{\delta}_2}{\overline{\delta}_1}$, boundary layer planar shape factor
L	body length
R	body radius
Re_L	$\frac{U_\infty L}{\nu}$, Reynolds number based on the body length
Re_V	$\frac{U_\infty V^{1/3}}{\nu}$, Reynolds number based on the body volume
$Re_{\overline{\delta}_2}$	$\frac{U\overline{\delta}_2}{\nu}$, Reynolds number based on the planar boundary-layer momentum thickness
r	R/L , non-dimensional body radius
r_i	the value of r at $x = x_i$
U	velocity component in the x direction at the edge of the boundary layer
U_∞	undisturbed free-stream velocity
u	boundary layer velocity component in the x direction
V	body volume
$\tilde{V}$	$\pi \int_0^1 (R/L)^2 \, d(x/L)$, body volume based on unit length

Nomenclature (Cont'd)

Symbol	Definition
v	boundary layer velocity component in the y direction
X	axial coordinate for the body
x	non-dimensional axial coordinate for the body
χ	Cartesian coordinate in the direction of the body surface (a coordinate for the boundary layer velocity field)
x_i	the i^{th} non-dimensional axial coordinate for the body
y	Cartesian coordinate in the direction normal to the surface of the body (a coordinate for the boundary layer velocity field)
α	coefficient in equations (16) and (17)
β	coefficient in equations (16) and (17)
Δ_1	$2\pi \int_0^\delta (1 - \frac{u}{U}) \rho \, dy$, boundary layer displacement area
Δ_2	$2\pi \int_0^\delta (1 - \frac{u}{U}) \frac{u}{U} \rho \, dy$, boundary layer momentum area
δ	boundary layer thickness
$\overline{\delta}_1$	$\int_0^\delta (1 - \frac{u}{U}) \, dy$, boundary layer planar displacement thickness
$\overline{\delta}_2$	$\int_0^\delta (1 - \frac{u}{U}) \frac{u}{U} \, dy$, boundary layer planar momentum thickness
θ	slope of the body at the tail
ν	kinematic viscosity of the fluid
ρ	distance to the body axis (a coordinate for the boundary layer velocity field)
$\overline{\rho}$	fluid density

1. Introduction

The design of low-drag bodies is a subject that hydrodynamicists and aerodynamicists have studied for years. It is clear that a reduction of drag for a given body will result in reduced requirements for propulsion systems and a greater range for a given fuel supply. In recent years, considerable research has been aimed at obtaining extensive regions of laminar flow to reduce the friction drag of incompressible bodies of revolution. Many factors affect the occurrence of transition from laminar to turbulent flow, including adverse pressure gradients, surface temperature and roughness, noise and turbulence present in the background media or generated by the propulsion system, and the use of suction to control the boundary layer velocity profile. In the design of a "laminar flow body" the objective is to use the effects to achieve as large a transition Reynolds number as possible for a practically shaped body. Unless special efforts are made in the design, manufacture, and maintenance of the body, underwater vehicles will experience boundary layer transition near the nose, and almost the entire surface will be covered by a turbulent boundary layer.

The principal question addressed by this study is whether significant drag reduction can be obtained for bodies of revolution by body shaping if it is assumed that the boundary layer becomes turbulent very near the nose. Previous work has been done on this problem. Gertler (1950) conducted a systematic experimental study of a family of streamlined bodies at the David Taylor Model Basin; this investigation is often referred to as the Series 58 study. Early work in airship design considered the drag of bodies of revolution (for example, Freeman (1932a) and Young (1939)); however, minimum-drag shapes, per se, were not studied. Parsons (1972) and Parsons, Goodson, and Goldschmeid (1974), using a boundary layer and potential flow computer program to calculate the drag, considered the application of numerical optimization methods to search for the shapes of low-drag bodies. Their study was primarily directed toward designing laminar flow bodies, although several calculations were made for all-turbulent boundary layers. Using a finite-difference boundary layer method, Hess and James (1975) also considered the possibility of low-drag, turbulent boundary layer bodies in their calculations of drag. The results of all the above studies indicate that the drag of an all-turbulent boundary layer body in incompressible flow is relatively

insensitive to body shape, provided the body is sufficiently streamlined to avoid separation. The question has arisen, however, as to whether these studies are conclusive and whether some more unconventional shape with a lower drag might exist.

In the study reported here, we have used numerical optimization methods to search for minimum-drag bcdies of revolution for incompressible flow and all-turbulent boundary layers. Although, our method is similar in spirit to that used by Parsons (1972), it is different in many respects. First, our optimization algorithm is the "method of feasible directions," which was used by Hicks, Murman, and Vanderplaats (1974) in the design of low-drag transonic airfoils. Second, the hydrodynamics program includes a potential flow method and an integral boundary layer method for computing the necessary parameters to evaluate the body drag. We decided that an integral boundary layer method would be sufficiently accurate and would require less computer time than a finite-difference boundary layer method. Third, we selected a new way of parameterizing the body shape, which specifies body ordinates at a discrete number of locations as the "design variables" and uses cubic splines under tension to define the body at other locations.

In the remaining sections of this report, the formulation of the problem, organization of the computer codes, and calculated examples are explained. In the discussion and conclusions section we observe two principal results of the study. First, using "state-of-the-art" potential flow and boundary layer methods and drag prediction formulas, we did not produce body shapes with significantly lower drag. We found one shape with significantly lower drag, but the drag formula used is questionable. Second, the "state-of-the-art" boundary layer methods are inaccurate in the aft body region, where the boundary layer is thick compared to the body radius. Boundary layer methods are inapplicable in this region because of the importance of radial pressure gradients and the interaction of the viscous and inviscid flow. For conventional bodies with high fineness ratios and thin boundary layers over most of the body, the inaccuracy in the tail region has little effect in the prediction of the total drag. However, for low-drag body shapes with smaller fineness ratios and thicker boundary layers, the inaccuracy in the tail region is significant. This observation has been independently observed in the recent note by Patel and Guven (1976). Good computational

models for this region are required before additional design studies are conducted.

Finally, we note that the basic optimization methods used in the present study may be employed in other design problems where the accuracy of the drag calculation is not a factor. Such studies include maximizing the transition Reynolds number by optimizing the surface temperature distribution for a given heating or cooling supply, optimizing suction distribution for a given pumping capacity, and maximizing the propulsion system efficiency.

2. Formulation of the Problem

2.1 Statement of the Problem

The problem is to find a body of revolution of prescribed volume, which has minimum drag at a given speed through a prescribed incompressible fluid. We assume that surface quality (in other words, roughness) promotes early transition of the boundary layer so that nearly the entire body surface has a turbulent boundary layer. Furthermore, we exclude bodies that have boundary layer separation.

We select the cube root of the volume $V^{1/3}$ as the reference length scale for the Reynolds number and for the drag coefficient, which are given respectively as

$$Re_V = \frac{U_\infty V^{1/3}}{\nu} , \tag{1}$$

$$C_{D_V} = \frac{D}{\frac{1}{2}\rho U_\infty^2 V^{2/3}} . \tag{2}$$

With this selection, the Reynolds number is fixed, and the drag coefficient is to be minimized during the search for an optimum body.

To make the problem tractable, we limit the search for an optimum body to a parameterized family of shapes. It is convenient to use the body length L as the length scale for defining the family non-dimensionally, and we write

$$R/L = f(X/L;a_1,a_2,\cdots a_n) \ , \ X = 0,L \ ,$$

$$R/L = 0 \ , \ X = 0 \ , \ X = L \ , \tag{3}$$

where a_i , $i = 1,n$ are free parameters. The two length scales, L and $V^{1/3}$, are related by the volume formula

$$V = \pi \int_0^L R^2 \, dX = L^3 \pi \int_0^1 (R/L)^2 \, d(X/L) = L^3 \tilde{V} , \tag{4}$$

where $\tilde{V}$ is the body volume for unit length given by

$$\tilde{V} = \pi \int_0^1 (R/L)^2 \, d(X/L) . \tag{5}$$

Since V is fixed and $\tilde{V}$ may be computed from the shape according to the preceding formula, there is only one independent length scale for the problem, and the other is directly related through the formula

$$L = (V/\tilde{V})^{1/3} \tag{6}$$

when the body shape is specified. In presenting the bodies, we plot all results using the variables X/L and R/L so that the bodies are all shown with unit length. The fatter bodies, however, will be physically shorter than the slender bodies for a fixed volume.

The problem under study may be formally stated in the following way: Given a body described by the equation

$$R/L = f(X/L;a_1,a_2,\cdots a_n) \ , \ X = 0,L$$

$$R = 0 \ , \ X = 0 \ , \ X = L \ , \tag{3}$$

where L is the length of the body, R is the radius, X is the axial coordinate, and a_i , $i = 1,n$ are free parameters, and given a method of computing the drag coefficient of the body for a specified Reynolds number and boundary layer transition point

$$C_{D_V} = F(R/L,Re_V) \ ,$$

find the values of a_i that minimize the drag coefficient, subject to various constraints. For the present problem the constraints selected are

(1) That the body have a nonnegative radius

$$R(X;a_1,a_2,\cdots a_n) > 0 \ , \ 0 < X < L \ , \tag{7}$$

(2) That the Reynolds number constant

$$Re_V = \frac{U_\infty V^{1/3}}{\nu} = \text{constant} \ , \tag{8}$$

which implies for a given speed and a given fluid (in other words, a given U_∞ and ν) that the volume be constant

$$V(a_1,a_2,\cdots a_n) = \pi \int_0^L R^2 \, dX = \text{constant} , \tag{9}$$

(3) That the boundary layer be turbulent (in other words, that the transition point be at the nose*), and

(4) That boundary layer separation does not occur on the body

$$C_f(X;a_1,a_2,\cdots a_n) \geq 0 , \; X = 0,L . \tag{10}$$

2.2 Optimization Method

The optimization method is basically a numerical search procedure in which we start with an initial body shape, and, by systematically altering the values of the design variables a_i, we reduce the objective function, the drag D, subject to the imposed constraints, until we reach a minimum value. This design method is a direct method because the body shape is specified, and the flow field and drag are calculated. Various numerical optimization methods are available. In this study, we used the "method of feasible directions," which was implemented by Vanderplaats (1973) and which has been successfully applied to problems involving the optimal shaping of transonic airfoils. A detailed explanation of the methodology is given by Vanderplaats, Hicks, and Murman (1975). The procedure is briefly outlined here.

With the initial values of the design variables a_i and the objective function D specified, we can calculate the gradient of D by using the following one-sided finite difference formulae

$$\frac{\partial D}{\partial a_i} = \frac{D(a_i,\cdots a_i+\Delta a_i,\cdots a_n) - D(a_i,\cdots a_i,\cdots a_n)}{\Delta a_i} , \; i = 1,n . \tag{11}$$

Assuming that no constraints are violated, we then proceed with our search for a minimum drag shape in the direction of steepest descent;

*In this study we approximated this condition by fixing transition at five percent of the length downstream from the nose.

that is, in the direction opposite to the gradient direction. Predetermined step sizes in the a_i space are used, and three steps are taken. The final step size is selected with the conjugate gradient method of Fletcher and Reeves (1964). After this step search is completed, the gradient of D is recalculated, and another search is done. Assuming that no constraints are violated in the process, this search procedure is continued until the change in drag in three successive searches is less than a specified convergence criteria.

If one or more constraints are violated (or nearly violated), then the gradient of the constraint is also calculated by finite-difference formulae, and the search proceeds in the direction that reduces the drag and avoids violating the constraint; that is, the "feasible direction." Again the search proceeds as above (without using the conjugate gradient method) until convergence is achieved or until it is determined that no feasible solution exists. Clearly, the final solution in either case may not be an absolute minimum. It may be a local minimum or, if the design space is "flat," the calculations may terminate because the convergence criterion is satisfied in three successive searches. In either case, however, if a significant reduction in drag is achieved, the method may be considered successful from an engineering viewpoint.

2.3 Body Parameterization

For the optimization method to be efficient, the body must be described by as few parameters as possible. On the other hand, for the optimization method to be general, the body parameterization method chosen must admit as diverse a set of shapes as possible. Thus, the selection of the body shape parameterization is an important part of the optimization calculation.

Several possible body parameterization methods were considered, but we actually tried only one. We list those considered since they may be useful for future optimization studies.

The simplest parameterization is a polynominal family

$$r^2 = \sum_{1}^{N} a_n x^n \ , \ 0 < x < 1 \qquad (12)$$

like the one used in the Series 58 study (Gertler, 1950). Hicks, Murman, and Vanderplaats (1974) used a similar family. A more versatile

adaptation of the polynominal representation are the linked polynomials

$$r^2 = \sum_1^N a_n x^n \ , \ 0 < x < x_1 \ ,$$

$$r^2 = \sum_1^M a_n x^n \ , \ x_1 < x < 1 \ . \qquad (13)$$

The use of different formulae on the front and back part of the body allows each region to be modified more independently. However, continuity of r and one or more of its derivatives is enforced at the match point x_1. Parsons (1972) and Vanderplaats, Hicks, and Murman (1975) used this procedure. Another possible method is to use super-ellipses

$$\left(\frac{x}{a}\right)^n + \left(\frac{r}{b}\right)^m = 1 \quad , \quad 0 < x < x_1 \ ,$$

$$\left(1 - \frac{x}{x_1}\right)^{n_1} + \left(\frac{r}{r_1}\right)^{m_1} = 1 \ , \ x_1 < x < 1 \ . \qquad (14)$$

A wide variety of shapes can be obtained by varying n , m , n_1 , and m_1 . A set of basis functions may also be employed, as follows:

$$r = \sum_1^N a_n f_n(x) \ , \ 0 < x < 1 \ , \qquad (15)$$

where the functions $f_n(x)$ are selected to have certain desirable properties. Hicks and Vanderplaats (1977) used this method very successfully in the design of low-drag airfoils.

The method used in this study is to choose the body radii r_i at a number of fixed locations x_i as the parameters and then to use a cubic-spline-under-tension interpolation method reported by Cline (1974) to describe the body at intermediate values of x . This method has the advantage that the body ordinates themselves become the design variables. The spline method requires that either the first or second derivatives of r be specified at the end point. Thus, for the tail point, we made the body slope θ a design variable. At the nose, however, the slope is generally infinite. In this region, we used the formula

$$r = \alpha x^{a_1} + \beta x \ , \ 0 < x < x_1 \qquad (16)$$

and matched the value of r and its first two derivatives at x_1 with the spline interpolation for the remainder of the body. In our early calculations (reported as Calculation No. 1 in section 4) we used the simpler formula

$$r = \alpha x^{a_1} , \quad 0 < x < x_1 \tag{17}$$

and matched only r and its first derivative at x_1. The matching with the spline determines α and β. The exponent a_1, however, remains free as a design variable, and a variety of nose bluntnesses are therefore possible. To summarize, for the present study, the design variables are the following:

nose bluntness factor	a_1
body radii	$r(x_i)$, $i = 1,N$
tail angle	θ

(18)

In the calculated examples, N is 5.

Two variations of the above method were considered but not tried. One variation is to allow the abscissa locations x_i to be design variables also. The other variation is to consider the perturbation from a fixed basic body shape. In this procedure, the initial body would be the basic body shape, and the perturbed radii would be the design variables. If the basic shape has a blunt nose, the special nose shape function, equation (16), would not be required.

2.4 Hydrodynamic Model

Once a body shape is specified, a hydrodynamic calculation must be performed to compute the drag. The drag arises from the viscous forces and may be separated into two components: (a) the shear stress or tangential force on the body, known as the friction drag; and (b) the normal stress or pressure force, known as the pressure drag. The sum of the pressure drag and the friction drag is the total or profile drag. This is the quantity we want to minimize.

The standard procedure for calculating the drag is to first calculate the inviscid flow with a potential flow method and, from this result, to

obtain the pressure distribution on the body. Next, with a boundary layer method, the viscous layer is calculated up to the separation point. Finally, the drag is evaluated from Young's (1939) or Granville's (1953) formula.

In the present study, several assumptions were made in assembling the hydrodynamics model. We assumed that for low-drag bodies, separation would not occur ahead of the tail, and therefore our viscous flow method did not need to treat separation. We also assumed that since we are principally interested in an integrated force — the drag, an integral boundary layer method would suffice and would be substantially faster than a finite-difference method. The results published by Hess and James (1975) support this assumption. The third assumption was that influence of the viscous flow region in the immediate vicinity of the tail would not substantially affect the overall drag, and, hence, a boundary layer method could be used along the entire length of the body even though it is incorrect in the tail region. This assumption was based on published methods for evaluating the drag with Young's and Granville's formula. Unfortunately, this assumption turned out to be the weak link in the hydrodynamics model, as we discuss later in this report. For low-drag bodies with thick boundary layers at the aft end, the breakdown of the boundary layer assumption is significant. The result has recently been reported by Patel and Guven (1976).

In the next section, we describe the actual boundary layer, potential flow, and drag formulae that were used. We note here, however, that two separate programs were employed. Computer Program No. 1 employs a potential flow method that Frank Woodward* developed by using a source distribution on the body surface according to the method of Hess and Smith (1966). The boundary layer method was developed by Frank Dvorak* using the Nash-Hicks (1968) integral method. Calculations performed with this program produced an interesting shape. The result, however, is questionable because of the thick boundary layer on the aft end. We therefore decided to use a program by Nakayama and Patel (1974), which is well documented and verified for traditional streamline body shapes. This program, referenced as Computer Program No. 2, was obtained directly from Professor Patel.

---

* Current Address: Analytical Methods, Inc., Bellevue, Washington.

3. The Computer Programs

A system for computing a body shape with minimum drag, according to the preceding discussion, has several well-delineated tasks:

(1) Parametrically defining the body shape,

(2) Calculating the potential flow,

(3) Calculating the boundary layer,

(4) Coupling the potential flow and boundary layer calculations,

(5) Calculating the drag, and

(6) Searching for the parameter values giving minimum drag.

Two computer programs were developed by assembling various codes available in the literature and at Flow Research Company. The flow diagrams shown in figures 1 and 2 show our choices for the tasks listed above.

3.1 Computer Program No. 1

Computer Program No. 1 uses the method of Hess and Smith (1966) for the potential flow calculation. The flow field is constructed with sources distributed on the body surface. The governing equation, a Fredholm integral equation of the second kind, enforces the desired normal velocity at the surface and is solved numerically by approximating the surface source distribution with constant-strength planar panels.

In Computer Program No. 1, the method of Nash and Hicks (1968) is used to calculate the growth of the turbulent boundary layer. It is based on the momentum and the moment of momentum integral relations for the boundary layer and on Cole's (1956) velocity profile family.

The potential flow and boundary layer calculations are coupled according to the traditional weak interaction approach. A potential flow is calculated to obtain a pressure distribution, which is then used for input to the boundary layer growth calculation. The potential-flow calculation is repeated with the boundary layer growth effects modeled by ejecting fluid from the body surface. The ejection velocity (in other words, the boundary condition for the potential flow calculation) is calculated according to the relation developed in appendix A. The new pressure distribution is used to repeat the boundary layer calculation. If greater accuracy is desired, the cycle may be repeated; however, for our purposes, additional iteration was not necessary.

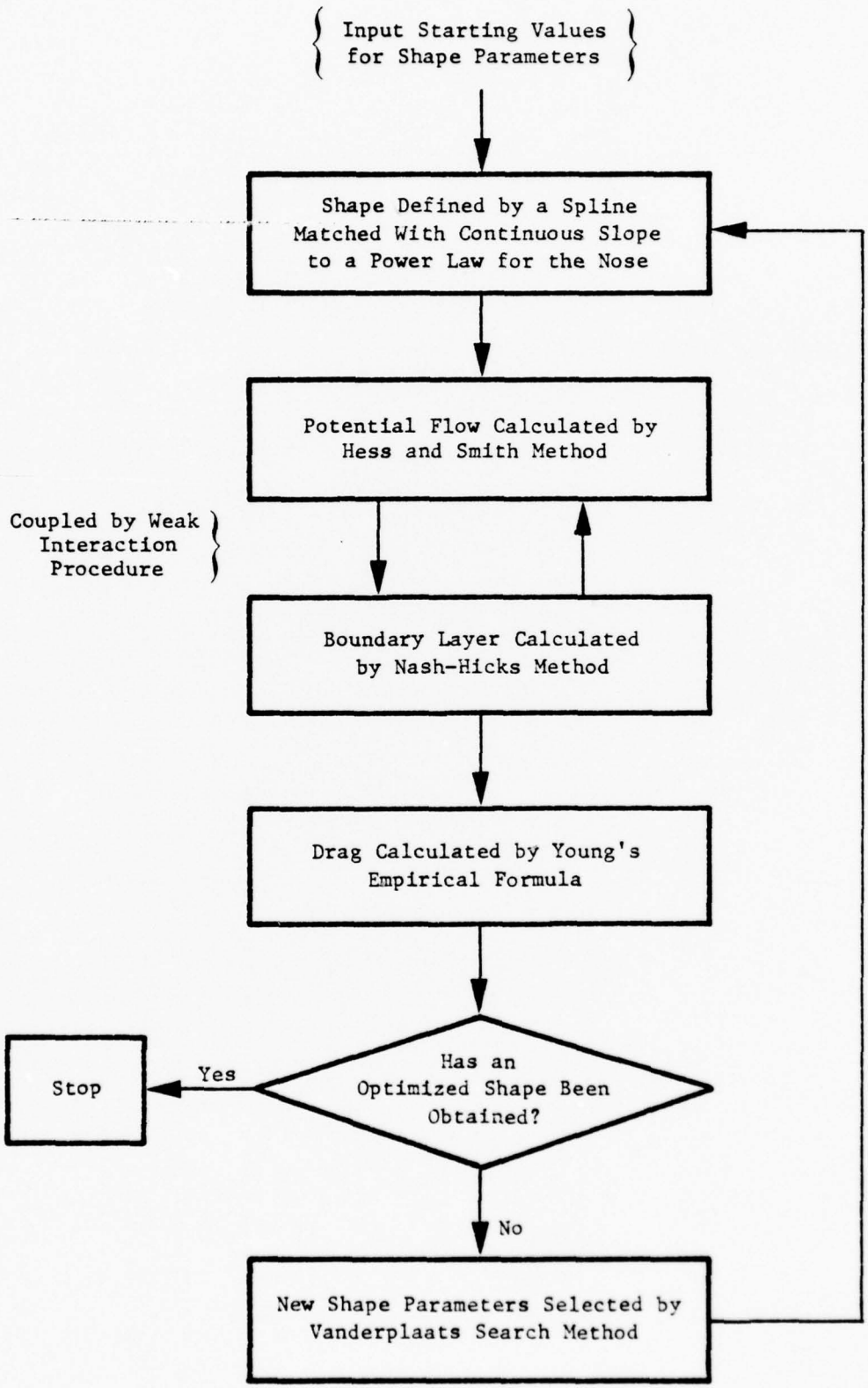

Figure 1 Flow Chart for Computer Program No. 1

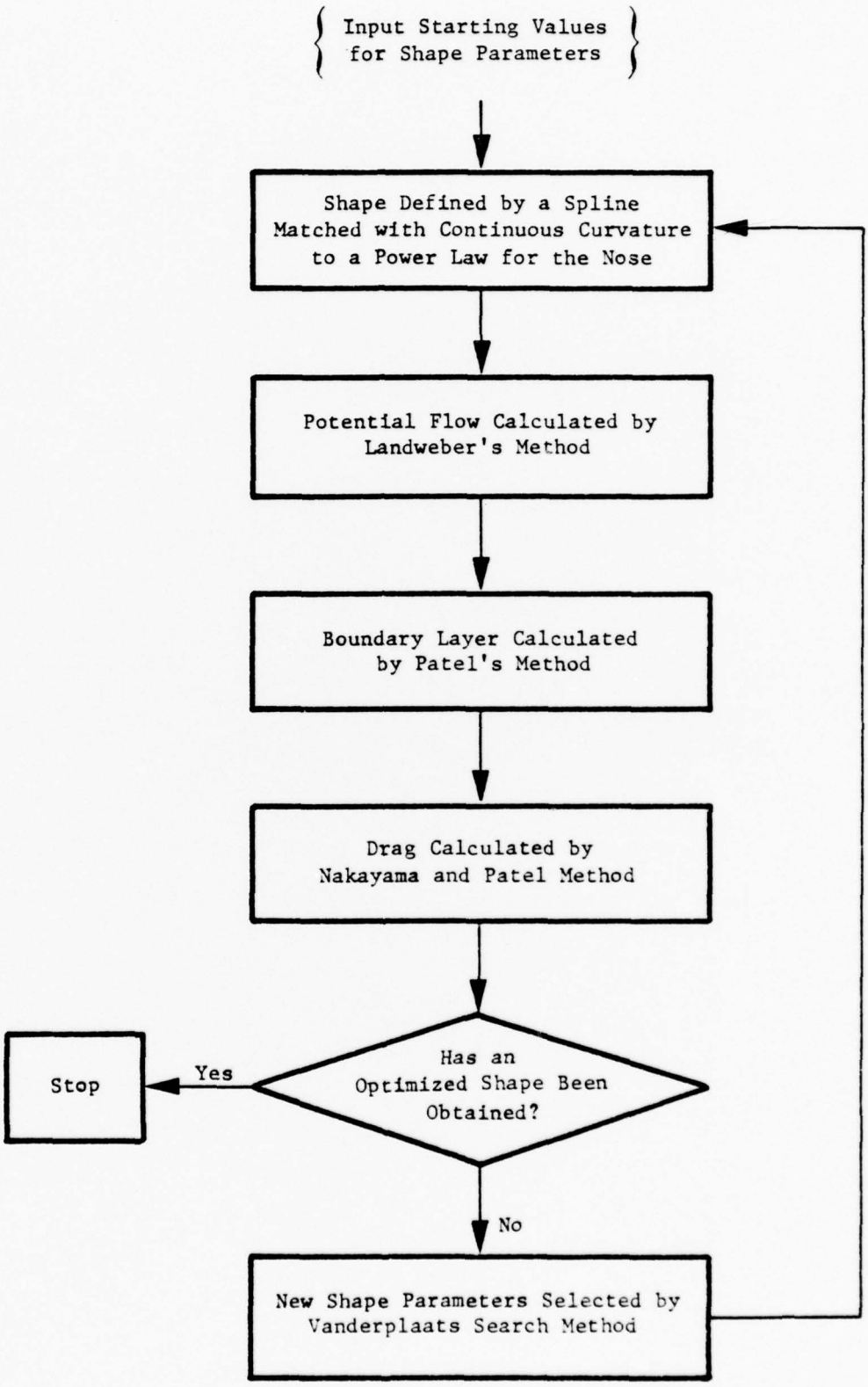

Figure 2 Flow Chart for Computer Program No. 2

To check the coupled boundary layer and potential flow calculation, we analyzed a body of revolution for which extensive experimental data were obtained by Yi and Przirembel (1973). The body that was tested was a long cylinder followed by an elliptical aftbody. This body could not be directly modeled in our calibration. Instead, we used a shortened body with three segments of equal length: the first segment was a 4 to 1 elliptical forebody, the second segment was a cylinder, and the third segment was a 4 to 1 elliptical aftbody. The initial development of the boundary layer was impossible to model since the experimental body extended upstream of the tunnel test section. Therefore, both the displacement and momentum thicknesses over the elliptical aftbody have smaller initial values in the computed results than the experimental data indicates. The shape factor, however, is almost correct, so this parameter, along with pressure coefficient, provided an adequate means of evaluation. Figure 3 shows the pressure coefficient and shape factor comparisons. For this calculation, separation was predicted, and the extrapolation of the normal ejection velocity beyond that point may explain the deviation of the calculated pressure from that measured near the tail. The shape factor agrees well in the region of decelerating flow.

To calculate the drag in Computer Program No. 1, we first compute the friction drag by integrating the surface shear stress from the boundary layer calculation, and we then use an empirical relation attributable to Young (1939). Young noted that theoretically derived pressure drags were approximately proportional to the thickness ratio and to the total drag, and he proposed the following formula:

$$C_{D_p} = 0.4(D/L)C_D \ , \tag{19}$$

where C_D is the total drag coefficient, C_{D_p} is the pressure drag coefficient, D is the maximum body diameter, and L is the body length. Using this relation we compute the total drag from the calculated friction drag according to

$$C_D = \frac{C_{D_f}}{1 - 0.4(D/L)} \ , \tag{20}$$

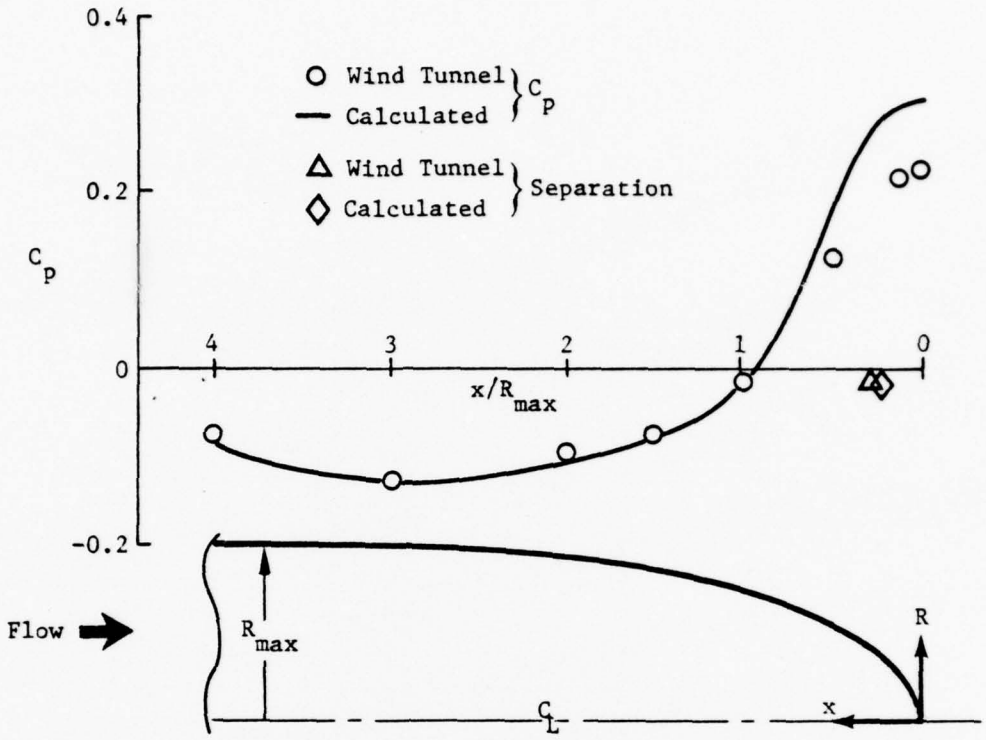

(a) Pressure Distribution

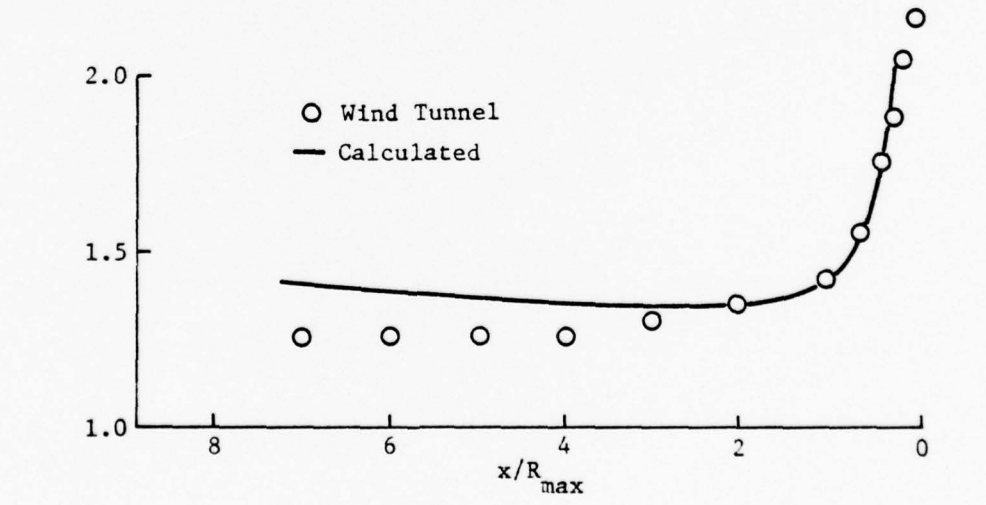

(b) Boundary Layer Growth

Figure 3 A Comparison of the Hydrodynamic Analysis Used in Computer Program No. 1 With a Wind Tunnel Test by Yi and Przirembel (1973)

where C_{D_f} is the skin friction drag coefficient. The advantage of using this simple formula is that the friction drag is accurately calculated by our method while the pressure drag is difficult to obtain by direct integration.

To assess the accuracy of the drag calculation method in Computer Program No. 1, we used it to compute the drag for six of the Series 58 bodies.[1] The comparison with the measured drag given in table 1 and figure 4 shows that the procedure is adequate for our purposes when the fineness ratio is seven or above. For the boundary layer calculations no iterations were made with the potential flow calculation to account for displacement thickness. To assure that the inaccurate drag calculations at low fineness ratio were not the result of this neglect, we repeated the calculation for the Model 4154 (fineness ratio 4), using one iteration. There was little change in the result.

Table 1

Series 58 Model No.	L/D Finess Ratio	C_{D_V}, Drag Coefficient at a Reynolds No. $Re_V = 2 \times 10^6$	
		Measured[2] Gertler (1950)	Computed by eq. (1)
4154	4	0.0197	0.0165
4155	5	0.0196	0.0176
4156	6	0.0197	0.0186
4165	7	0.0206	0.0202
4158	8	0.0221	0.0216
4159	10	0.0198	0.0195

[1] We refer frequently to the Series 58 bodies, which are a family of shapes tested at the David Taylor Model Basin and reported by Gertler (1950).

[2] A trip strip five percent of the length downstream from the nose provided a turbulent boundary layer.

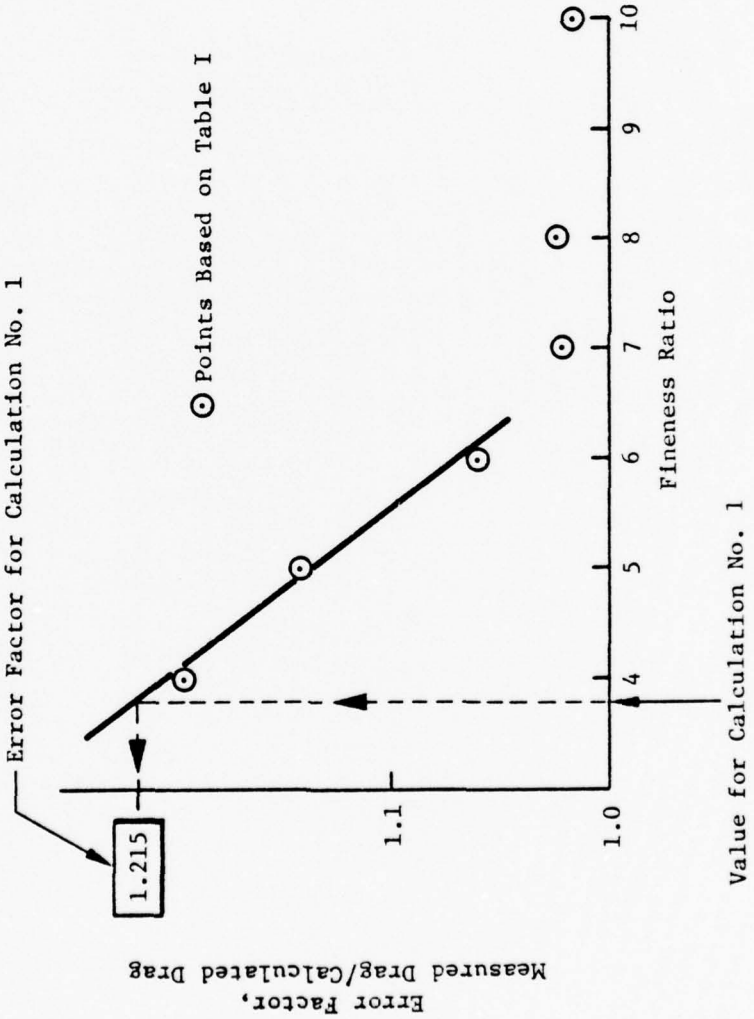

Figure 4 Drag Error Factor Based on Table I

The standard procedure for calculating drag based on the well-known Squire-Young formula was discarded after making some comparisons with experiment as described in the following. The formula given by Young (1939) for this procedure is

$$C_D = \frac{2\Delta_2}{A} \left(\frac{U}{U_\infty}\right)^{\frac{H+5}{2}} , \qquad (21)$$

where A is the reference area for the drag coefficient C_D, and where the following are evaluated at the tail of the body:

Δ_2 = the boundary layer momentum area,

U = the velocity at the edge of the boundary layer, and

H = the boundary layer shape factor .

Using the pressure distribution measured in the Langley 20-foot propeller research tunnel for the Airship Akron and reported by Freeman (1932b), we calculated the boundary layer growth and then computed the drag, first according to equation (20) and then according to equation (21). The comparison with the measured drag reported by Freeman (1932b) is given in table 2. For a second comparison, we analyzed Model 4165 of the Series 58 bodies with our potential flow and boundary layer computer programs without any iterations to add boundary-layer displacement thickness. We then computed the drag according to equations (20) and (21). Comparison with the measured drag reported by Gertler (1950) is given in table 2. The unreliable predictions obtained with equation (21) do not necessarily invalidate the equation. They may be caused by inaccurate values used for the boundary layer properties at the end of the body. This region is the most inaccurate for the boundary layer calculation. On the other hand, the results of equation (20) are not sensitive to the inaccuracies of the boundary layer calculation in this region since the contribution to the skin friction from the aft end is small.

Table 2

Model	Length Reynolds Number	Drag Coefficient C_{D_V}		
		Measured Freeman (1932b) Gertler (1950)	Equation (20)	Equation (21)
U.S. Akron	12.3×10^6	0.0198[1]	0.0198	0.0391
Series 58 Model 4165	10.0×10^6	0.0220[2]	0.0219	0.0601

As indicated in figure 1, the parameterized family of shapes used for Computer Program No. 1 consists of a nose relation and a cubic spline matched with continuous slope but not curvature. Thus, the quantity β in equation (16) was set to zero, the quantity α was determined so as to give continuity in radius at the match point, and the spline was forced to have the slope of the nose shape at the match point (see figure 5).

The resulting free parameters are the exponent a_1 in the nose relation

$$r = \alpha x^{a_1} , \tag{17}$$

the radii at the spline points, except for the tail point (this radius was fixed at zero), and the slope at the tail. This parametric definition provides a diverse family of shapes, including some with blunt noses (in other words, those with $a_1 < 1$).

[1] Boundary layer transition was measured to be about seven percent of the length downstream from the nose.

[2] A trip strip five percent of the length downstream from the nose provided a turbulent boundary layer.

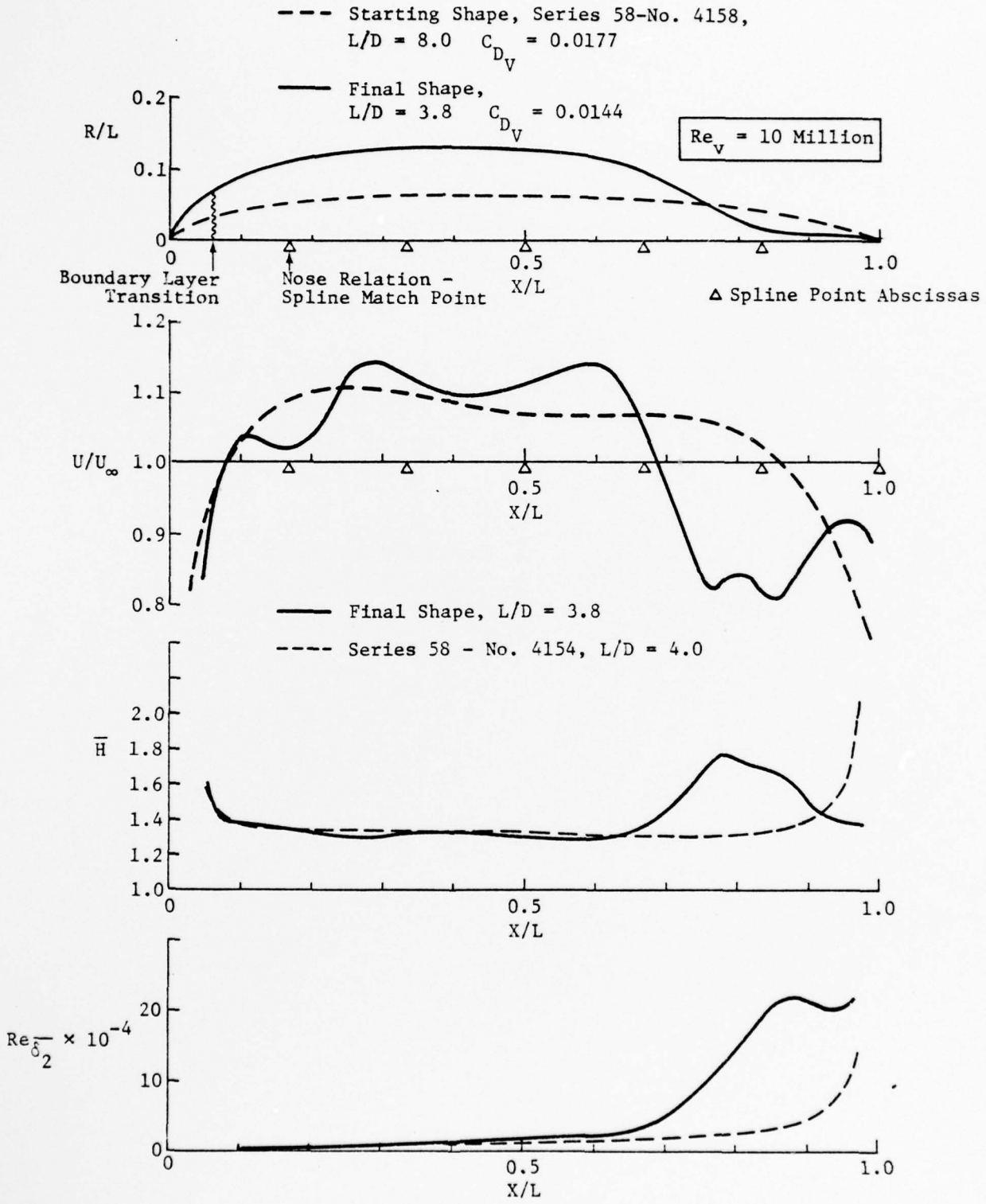

Figure 5 Minimum Drag Body Calculated by Computer Program No. 1, Including a Comparison of Its Boundary Characteristics With Those of a Series 58 Body With Nearly the Same Fineness Ratio

3.2 Computer Program No. 2

The fluid mechanical calculations for Computer Program No. 2 are based entirely on the methods used by Nakayama and Patel (1974). The potential flow is calculated by the method of Landweber (1959), and the flow field is constructed with doublets distributed on the axis of symmetry. The governing equation, a Fredholm integral equation of the first kind, enforces flow tangency at the body surface. It is solved by iteration with numerical evaluation (by Gauss quadrature) of the integral appearing in the equation.

The turbulent boundary layer calculation method in Computer Program No. 2 was developed by Patel (1974). It uses power-law velocity profiles in a momentum integral relation, and, for auxiliary relations, it uses an appropriate skin-friction law and an entrainment equation.

The drag is calculated in Program No. 2 according to the method of Nakayama and Patel (1974), and the explanation given in the reference is repeated here for convenience. The potential flow is calculated without boundary layer displacement modeling to obtain the pressure distribution for the boundary layer calculation. After each step in the boundary layer calculation over the last ten percent of the body, the drag formula of Granville (1953), (a modification of equation (21)),

$$C_D \approx \frac{2\Delta_2}{A} \left(\frac{U}{U_\infty}\right)^{\frac{7H+17}{8}} \tag{22}$$

is applied to determine a "local drag coefficient." The successive values of this drag coefficient increase up to some point and decrease as the boundary layer calculation approaches the tail of the body. Instead of using the value at the tail end, as indicated by the original Squire-Young drag method, Nakayama and Patel take the drag coefficient simply to be the maximum value. Comparisons of the drag computed in this manner with experiment are given by the authors and support the acceptability of this procedure for traditionally shaped bodies. A recent note by Patel and Guven (1976) reports that this method is not reliable for bodies with thick aft-end boundary layers and low fineness ratios.

For Computer Program No. 2, the parameterization of the shapes is the same as that used for Computer Program No. 1, except that continuity

through the second derivative is enforced at the match point between the nose relation and the cubic spline. Thus, the full nose relation

$$r = \alpha x^{a_1} + \beta x \tag{16}$$

is used, and the quantities α and β are determined by the continuity requirements.

4. Calculated Examples

One example calculation using Computer Program No. 1 and two calculations using Computer Program No. 2 are presented in the following. The Reynolds number based on the cube root of the volume is ten million for all of the examples; in other words, $Re_V = 10^7$. Also, the boundary-layer transition point was fixed at the five percent body station (X/L = 0.05) for all calculations.

For each calculation the starting and final shapes are illustrated, and, for the final shapes, plots of the boundary-layer edge velocity U , the planar shape factor $\overline{H}$, and the planar momentum thickness Reynolds number $R_{\overline{\delta}_2}$, as calculated by the hydrodynamics part of the computer programs, are presented.

4.1 Calculation No. 1

For the first calculation we used Computer Program No. 1, starting with the Series 58, Model No. 4158 body shape. The spline point abscissas were equally spaced along the x axis, as shown in figure 5. Therefore, the seven parameters varied during the optimization search were the exponent of the nose relation

$$r = \alpha x^{a_1} , \tag{17}$$

which extended from $x = 0$ to $x = 1/6$, the radii at

$$x = 1/6,\ 2/6,\ 3/6,\ 4/6,\ 5/6 ,$$

and the slope at the tail.

As mentioned earlier, the potential flow solution involves approximating a surface source distribution with constant-strength source panels. For Calculation No. 1 we obtained the paneling by equally dividing the axial coordinate from the nose to the tail and by equally dividing the polar coordinate, associated with a body of revolution, from 0 to 2π . For both directions, the number of divisions was chosen to be 20.

The calculated drag of the starting shape was

$$C_{D_V}{}_{start} = 0.0177 ,$$

and the measured drag was reported by Gertler (1950) to be

$$C_{D_V} = 0.0180 .$$

The resulting minimum drag shape is shown in figure 5 together with the starting shape. The calculated drag for the final shape was

$$C_{D_V}{}_{final} = 0.0144 .$$

The final shape is characterized by a low fineness ratio (3.8, compared to 8.0 for the starting shape) and a delayed and severe convergence to the tail point.

Also in figure 5 we compare the boundary-layer properties for the final shape to those for a Series 58 body having about the same fineness ratio. We obtained these results from the hydrodynamics part of Computer Program No. 1.

We note here two features of the velocity distribution shown in figure 5. The dip in the velocity at $X/L = 0.18$ is associated with a discontinuity in curvature, which occurs where the nose relation is matched to the cubic spline. For the calculations with Computer Program No. 2, for which curvature is continuous everywhere, irregularity at this match point did not appear. The second irregularity in the velocity distribution in figure 5 occurs near the tail. The streamwise panel length used for the numerical approximation to the surface source distribution for the potential flow calculation is larger than the radius over the last twenty-five percent of the body length (for example, at $X/L = 0.90$ the panel length is five times the radius). We believe that this coarse paneling is responsible for the velocity irregularity in this region. This irregularity did not occur in Calculation No. 3, where the same shape was analyzed (as the starting shape) by Computer Program No. 2 using a more appropriate discretization for the numerical solution to the potential flow problem (see section 4.3).

Table 3

Calculation		C_{D_V}	$Re_L \times 10^{-6}$	L/D
Computer Program No. 1	Starting Shape (Model 4158)	0.0177	50	8.0
	Final Shape	0.0144	32	3.8
Computer Program No. 2	Starting Shape (Model 4158)	0.0180	50	8.0
	Final Shape	0.0174	43	5.7

4.2 Calculation No. 2

For Calculation No. 2 we repeated Calculation No. 1 with the following changes. Computer Program No. 2 was used, and the spline point abscissas were changed to decrease their spacing at the front part of the body, as shown in figure 6. Thus, the seven parameters varied during the search procedure were the exponenent of the nose relation

$$r = \alpha x^{a_1} + \beta x \ , \tag{16}$$

which extended from $x = 0$ to $x = 0.075$, the radii at

$$x = 0.075,\ 0.225,\ 0.425,\ 0.625,\ 0.824 \ ,$$

and the slope at the tail.

For the potential flow calculation the order of the Gauss quadrature formula used to evaluate the integral in the governing equation was chosen to be 24.

For this calculation, the drags for the starting and final shapes were

$$C_{D_V}{}_{start} = 0.0180$$

and

$$C_{D_V}{}_{final} = 0.0174 \ ,$$

and the starting and final shapes and the final boundary-layer properties are shown in figure 6. The search increased the maximum thickness of the shape somewhat and moved the point of maximum thickness forward. Table 3 summarizes comparisons of the first two calculations.

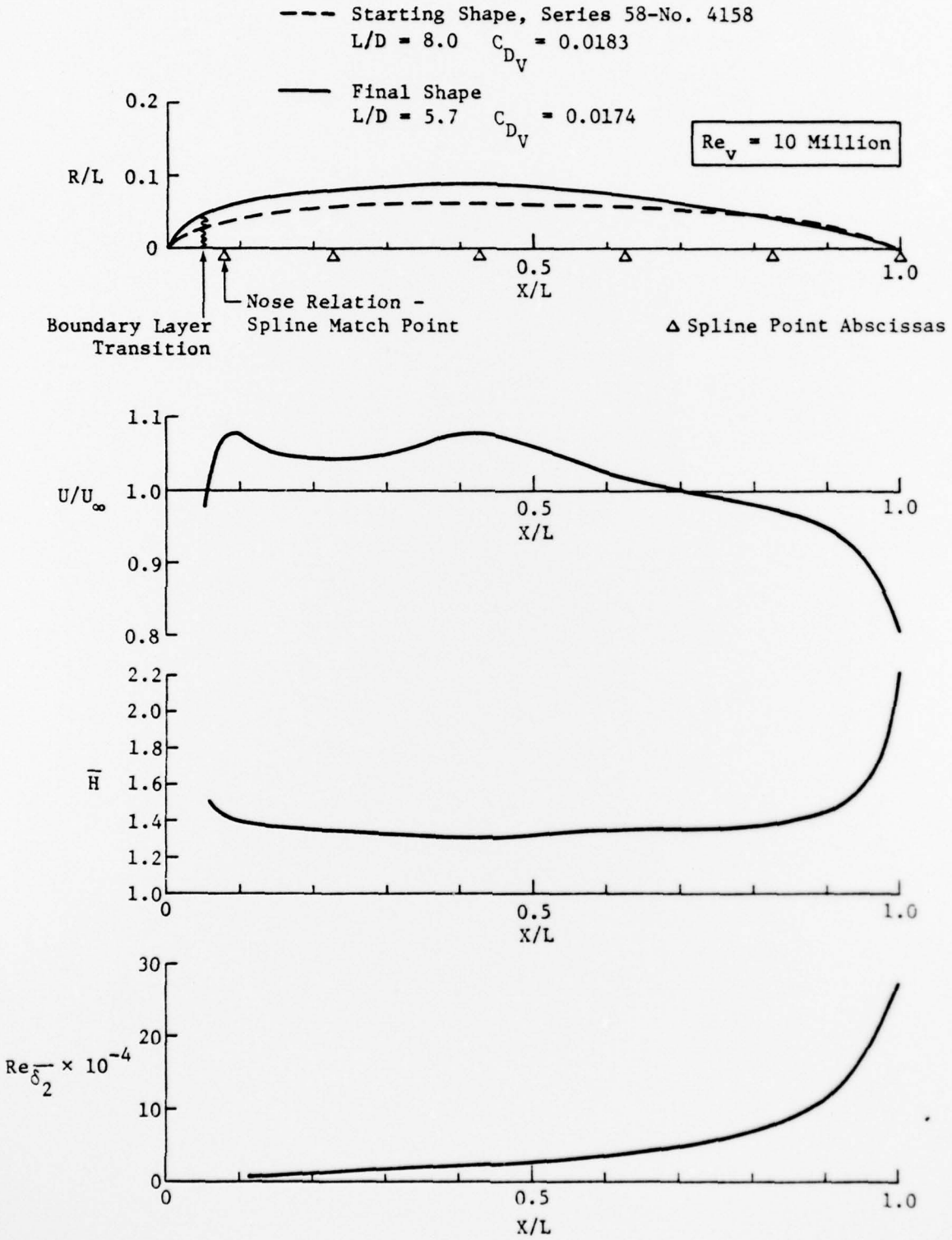

Figure 6 Minimum Drag Body and Boundary Layer Characteristics Calculated by Computer Program No. 2, With the Same Starting Body as for the Calculation Made With Computer Program No. 1.

4.3 Calculation No. 3

Since the results of Calculations Nos. 1 and 2 are so markedly different, we thought it would be interesting to investigate the importance of the starting shape on the final result. For this reason, we used the unorthodox shape obtained as a minimum drag body by Computer Program No. 1 as a starting shape for Calculation No. 3, using Computer Program No. 2. We used the same set of spline point abscissas for both calculations, as indicated in figures 5 and 7. Also, as in Calculation No. 2, the order of the Gauss quadrature was 24 for the potential flow calculation.

The results of Calculation No. 3 are shown in figure 7. Note that the drag for the starting shape is considerably higher than the value computed by Computer Program No. 1:

$$C_{D_{V_{start}}} = \begin{cases} 0.0144 & \text{for Computer Program No. 1} \\ 0.0186 & \text{for Computer Program No. 2} \end{cases} .$$

Also of interest is that the final shape, although considerably thicker than that for Calculation No. 2, has nearly the same drag:

$$C_{D_V} = \begin{cases} 0.0174 & \text{for the optimized value from Calculation No. 2} \\ 0.0172 & \text{for the optimized value from Calculation No. 3} \end{cases} .$$

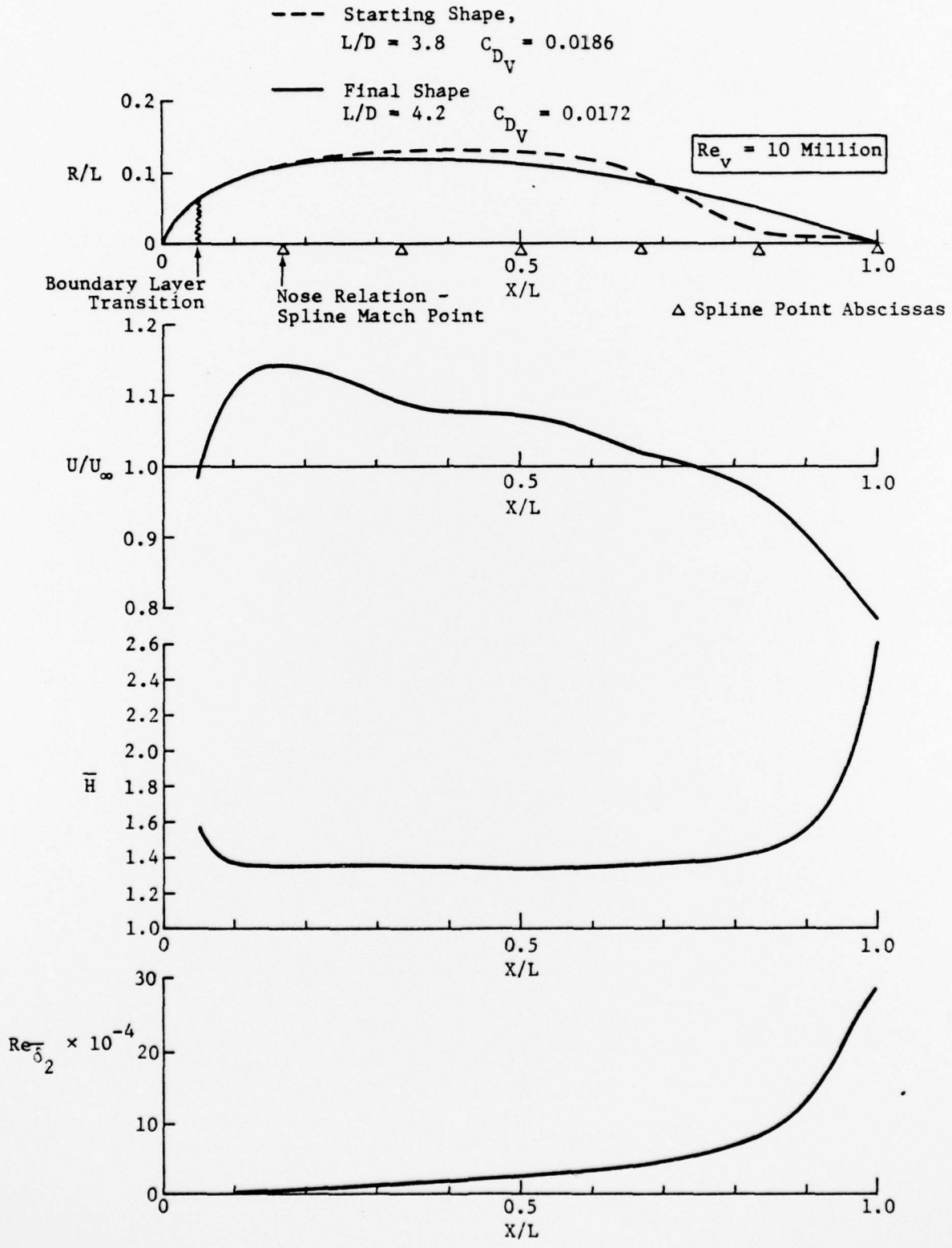

Figure 7 Minimum Drag Body and Boundary Layer Characteristics Calculated by Computer Program No. 2, Starting With the Minimum Drag Body Calculated by Computer Program No. 1.

5. Discussion and Conclusions

The optimization calculation using Computer Program No. 1 produced a thick body (fineness ratio 3.8) with a drag 19 percent lower than that for the Series 58, Model 4158 body, a conventional shape with a fineness ratio of 8 and the shape used to initiate the optimization search. According to the check cases discussed in section 3.1, the drag model used in Computer Program No. 1 underpredicts the drag for low fineness ratios. Figure 4, based on the information in Table 1 of that section, gives the discrepancy between calculated and measured drags as a function of the fineness ratio. Although the applicability of this plot to other shapes is not established, it is useful for making rough corrections, and, if applied to the results of the optimized shape obtained by Computer Program No. 1 (see figure 5), the drag is increased to

$$C_{D_V} = 0.0175 \quad ,$$

which is nearly the same as for the starting shape.

We expect from the results shown in table 1 of section 3.1 that the optimization search would lead to a low fineness ratio. It is unfortunate that the low drag calculated is apparently the result of the inadequacy of the drag model used and not the result of a superior shape. It was primarily because of this inadequacy that we developed Computer Program No. 2. We note, however, that the optimization method performed satisfactorily; it successfully found a lower drag body.

Computer Program No. 2 is based on the method of Nakayama and Patel (1974), which is generally regarded as the best state-of-the-art drag prediction method using an integral boundary-layer procedure (for example, see Hess and James (1975)).

The optimization calculations with Computer Program No. 2 support the conclusion that shaping alone cannot significantly reduce the drag below that of the conventional shapes exemplified by the Series 58 bodies. In fact, the two optimized shapes calculated had drags of only five to six percent less than for Model 4158 of Series 58. The conclusion that the drag is insensitive to a shape perturbation from a streamlined unseparated body when the boundary-layer is turbulent over most of the wetted surface agrees with previous investigations;

for example, that of Hess and James (1975). We note, however, that for the unusual starting shape used in Calculation No. 3, the drag model predicts a drag significantly higher than that of traditional shapes, and the optimization search successfully drives the shape toward a conventional one.

We also note that the boundary layer shape factor H never exceeded 1.82 for the final shapes obtained by Computer Program No. 2. The highest value occurred at the tail for Calculation No. 3 and corresponds to a value of 2.59 for the planar shape factor $\bar{H}$, as indicated in figure 7. Thus, boundary layer separation would not be expected for these shapes, and the inability of the program to predict separation and calculate the associated drag is therefore unimportant.

If we had used more accurate methods to calculate the drag, we may have been able to show more significant drag reduction by shaping than was demonstrated in this study. The example calculations based on best state-of-the-art drag prediction method using an integral boundary layer procedure indicated that the drags of bodies with all-turbulent, unseparated boundary layers do not differ greatly. However, the drag calculations that lead to this conclusion rely on the formula of Granville (1953, see equation (22)), which requires an evaluation of the boundary layer momentum area at the tail. Since standard boundary layer calculations are not valid near the tail, it is difficult to apply this formula. Furthermore, recent observations by Patel and Guven (1976) show that the Granville formula gives appreciable error when the tail boundary layer is unseparated but thick. The breakdown of the boundary layer calculation and the Granville drag formula results from neglect of radial pressure gradients. In addition, thin boundary layer approximations are violated. It appears that more sophisticated numerical methods (for example, finite-difference calculations) must be used to calculate the drag with a high degree of accuracy. These methods must allow for the following:

(1) The boundary layer thickness is not assumed to be small compared to the body radius,

(2) The pressure gradient normal to the surface is not neglected, and

(3) The viscous-inviscid flow interaction is adequately represented.

We believe that more accurate drag calculations incorporating the above items should be developed. Such methods would be useful for calculating the turbulent aft-end region of laminar flow bodies, as well as all-turbulent boundary layer bodies.

References

Cline, A. K. (1974) "Algorithm 476 - Six Subprograms for Curve Fitting Using Splines Under Tension," Communication of the ACM 17, no. 4. April.

Cole, D. E. (1956) "The Law of the Wake in the Turbulent Boundary Layer," J. Fluid Mech. 1.

Fletcher, R. and Reeves, C. M. (1964) "Function Minimization by Conjugate Gradients," Brit. Computer J. 7, no. 2.

Freeman, H. B. (1932a) "Measurements of Flow in the Boundary Layer of a 1/40-Scale Model of the U.S. Airship Akron," NACA TR 430.

Freeman, H. B. (1932b) "Force Measurements on a 1/40-Scale Model of the U.S. Airship Akron," NACA TR 432.

Gertler, M. (1950) "Resistance Experiments on a Systematic Series of Streamlined Bodies of Revolution - For Application to the Design of High Speed Submarines," Report C-297, David Taylor Model Basin, Naval Ship Research and Development Center, Washington, D.C.

Granville, P. S. (1953) "The Calculation of Viscous Drag of Bodies of Revolution," Rept. 849, David Taylor Model Basin, Washington, D.C.

Hess, J. L. and James, R. M. (1975) "On the Problem of Shaping an Axisymmetric Body To Obtain Low Drag at Large Reynolds Number," Douglas Aircraft Co. Report No. MDC J6791, January.

Hess, J. L. and Smith, M. M. U. (1966) "Calculation of Potential Flow About Arbitrary Bodies," Progress in Aeronautical Sciences Series, vol. 8, Permagon Press, New York.

Hicks, R. M., Murman, E. M., and Vanderplaats, G. N. (1974) "An Assessment of Airfoil Design by Numerical Optimization," NASA TM X-3092, July.

Hicks, R. M. and Vanderplaats, G. N. (1977) "Application of Numerical Optimization to Design of Supercritical Airfoils Without Drag Creep," SAE Paper 770440.

Landweber, L. (1959) "Potential Flow About Bodies of Revolution and Symmetric Two-Dimensional Flows," BuShips Index NS715-102, Iowa Institute of Hydraulic Research, Iowa City, Iowa.

Nakayama, A. and Patel, V. C. (1974) "Calculation of the Viscous Resistance of Bodies of Revolution," J. Hydronautics, 154-162, October.

Nakayama, A., Patel, V. C., and Landweber, L. (1976) "Flow Interaction Near the Tail of a Body of Revolution, Part II: Iterative Solution for Flow Within and Exterior to Boundary Layer and Wake," J. Fl. Eng., Trans. ASME, Series I, vol. 98, no. 3, September.

References (Cont'd)

Nash, J. F. and Hicks, S. G. (1968) "An Integral Method Including the Effects of Upstream History on the Turbulent Shear Stress," Proceedings - Computation of Turbulent Boundary Layers, AFOSR-IFP-Stanford Conference, vol. 1, Stanford University Dept. Mech. Eng., Stanford, California.

Parsons, J. S. (1972) "The Optimum Shaping of Axisymmetric Bodies for Minimum Drag in Incompressible Flow," Ph.D Thesis, School of Mechanical Engineering, Purdue University, Lafayette, Indiana.

Parsons, J. S., Goodsen, R. E., and Goldschmied, F. R. (1974) "Shaping of Axisymmetric Bodies for Minimum Drag in Incompressible Flow," J. Hydronautics 8, July.

Patel, V. C. (1974) "A Simple Integral Method for the Calculation of Thick Axisymmetric Turbulent Boundary Layers," Aeron. Quart. 25, 47-58.

Patel, V. C. and Guven, O. (1976) "Importance of the Near Wake in Drag Prediction of Bodies of Revolution," AIAA J. 14, no. 8, August.

Vanderplaats, G. N. (1973) "CONMIN - A Fortran Program for Constrained Function Minimization, User's Manual," NASA TM X, 62, 282, August.

Vanderplaats, G. N., Hicks, R. M., and Murman, E. M. (1975) "Application of Numerical Optimization Techniques to Airfoil Design," NASA SP 347, 749-768.

Yi, C. H. and Przirembel, C. (1973) "Incompressible Turbulent Boundary Layer Separation From a Curved Axisymmetric Body," Developments in Mechanics 7, Proceedings of the 13th Midwestern Conference, M73, 203-216.

Young, A. D. (1939) "The Calculation of the Total and Skin Friction Drags of Revolution at Zero Incidence," R & M 1874, Aeronautical Research Council, London, England.

Appendix A: The Potential Flow Boundary Condition Required To Simulate Boundary Layer Displacement

There are two methods to account for the displacement of the boundary layer when obtaining the potential flow solution. One method is to displace the surface, and the other is to eject fluid from the surface (in other words, to prescribe a surface normal component for the velocity at the wall). In the following we develop an equation for the latter in terms of the boundary layer growth. Important quantities are defined in figure A-1. Note that the x and y directions refer to wall tangential and normal direction, respectively.

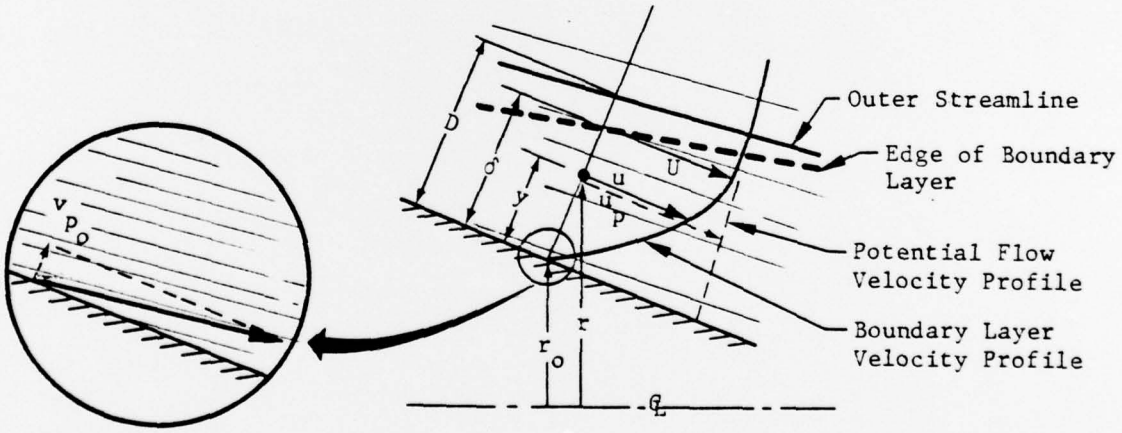

Figure A-1 Nomenclature

Two velocity fields are relevant. The first is that the velocity field for the real flow (with a boundary layer) for which the x and y components of velocity are denoted by u and v, respectively. For this field, the velocity vanishes at the surface, and the tangential velocity at the edge of the boundary layer is denoted by U. The second velocity field considered is a potential flow that matches the real flow outside the boundary layer. Its components are denoted by u_p and v_p and differ from u and v in the boundary layer region only.

Note also in figure A-1 that the edge of the boundary layer, a distance δ above the surface, is not a streamline. We will consider some streamline just outside the boundary layer, which we call the outer streamline. Its distance above the surface is denoted by D.

For the real flow field, the volume flux under the outer streamline is

$$Q = \int_o^D u 2\pi r \, dy = \int_o^D 2\pi U r \, dy - \int_o^D 2\pi (U - u) r \, dy .$$

Conservation of mass requires that

$$\frac{dQ}{dx} = 0 ,$$

so that

$$\frac{d}{dx} \int_o^D 2\pi U r \, dy - \frac{d}{dx} \int_o^D 2\pi (U - u) r \, dy = 0 .$$

For the potential flow, the volume flux under the outer streamline is

$$Q_p = \int_o^D u_p 2\pi r \, dy = \int_o^D 2\pi U r \, dy - \int_o^D 2\pi (U - u_p) r \, dy .$$

Conservation of mass requires that

$$\frac{dQ_p}{dx} = 2\pi r_o v_{p_o} ,$$

where r_o = surface radius

v_{p_o} = normal velocity component of the potential flow at the surface.

Thus,

$$\frac{d}{dx}\int_o^D 2\pi U r\, dy - \frac{d}{dx}\int_o^D 2\pi(U - u_p) r\, dy = 2\pi r_o v_{p_o} .$$

Subtracting the conservation of mass equations for the two velocity fields while noting that

$$u_p = u \quad \text{for} \quad y \geq \delta$$

gives

$$\frac{d}{dx}\left[\int_o^\delta 2\pi(U - u) r\, dy - \int_o^\delta 2\pi(U - u_p) r\, dy\right] = 2\pi r_o v_{p_o} .$$

We assume that the potential flow velocity does not vary significantly from $y = 0$ to $y = \delta$ so

$$u_p \doteq \left[u_p\right]_{y = \delta} = U ,$$

and, therefore, the second integral on the left-hand side of the above equation is small compared to the first. Thus, the normal component of velocity at the surface for the potential flow that simulates the boundary layer displacement is approximately

$$v_{p_o} = \frac{1}{2\pi r_o}\frac{d}{dx}\int_o^\delta 2\pi(U - u) r\, dy = \frac{1}{2\pi r_o}\frac{d}{dx}(U\Delta_1) ,$$

where the boundary layer displacement area Δ_1 is defined by

$$\Delta_1 = 2\pi\int_o^\delta (1 - \frac{u}{U}) r\, dy .$$